

## Electronic Supplementary Information

### **An electrochemically fabricated cobalt iron oxyhydroxide bifunctional electrode for an anion exchange membrane water electrolyzer**

Seokjin Hong<sup>a,1</sup>, Hyunki Kim<sup>a,1</sup>, Ho Won Jang<sup>b,\*</sup>, Soo Young Kim<sup>c,\*</sup>, and Sang Hyun Ahn<sup>a,\*</sup>

<sup>a</sup>*School of Chemical Engineering and Material Science, Chung-Ang University, Seoul 06974, Republic of Korea*

<sup>b</sup>*Department of Materials Science and Engineering, Research Institute of Advanced Materials, Seoul National University, Seoul 08826, Republic of Korea*

<sup>c</sup>*Department of Materials Science and Engineering, Korea University, Seoul 02841, Republic of Korea*

\*Corresponding authors.

E-mail: shahn@cau.ac.kr (Sang Hyun Ahn), sooyoungkim@korea.ac.kr (Soo Young Kim),

hwjang@snu.ac.kr (Ho Won Jang)

<sup>1</sup>These authors contributed equally to this work.

**Table S1** Electrodeposition condition of of  $\text{CoO}_x\text{H}_y/\text{TP}$ ,  $\text{Co}_z\text{Fe}_{1-z}\text{O}_x\text{H}_y/\text{TP}$ , and  $\text{FeO}_x\text{H}_y/\text{TP}$ 

Electrodes	Electrolyte concentration (mM)				Deposition conditions	
	$\text{CoSO}_4 \cdot 7\text{H}_2\text{O}$	$\text{FeSO}_4 \cdot 7\text{H}_2\text{O}$	$\text{Na}_2\text{SO}_4$	$\text{Na}_3\text{C}_6\text{H}_5\text{O}_7$	Potential ( $V_{\text{SCE}}$ )	Time (s)
$\text{CoO}_x\text{H}_y/\text{TP}$	35.0	-	100.0	100.0	-1.8	600.0
$\text{Co}_{65}\text{Fe}_{35}\text{O}_x\text{H}_y/\text{TP}$	30.0	5.0	100.0	100.0	-1.8	600.0
$\text{Co}_{52}\text{Fe}_{48}\text{O}_x\text{H}_y/\text{TP}$	17.5	17.5	100.0	100.0	-1.8	600.0
$\text{Co}_{47}\text{Fe}_{53}\text{O}_x\text{H}_y/\text{TP}$	10.0	25.0	100.0	100.0	-1.8	600.0
$\text{FeO}_x\text{H}_y/\text{TP}$	-	35.0	100.0	100.0	-1.8	600.0

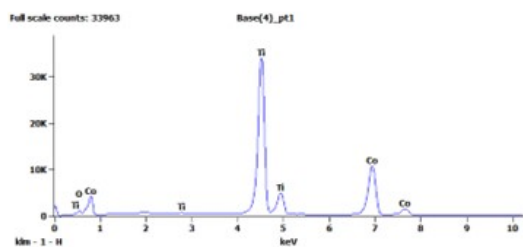
**Table S2** HER and OER performances of  $\text{CoO}_x\text{H}_y/\text{TP}$ ,  $\text{Co}_z\text{Fe}_{1-z}\text{O}_x\text{H}_y/\text{TP}$ , and  $\text{FeO}_x\text{H}_y/\text{TP}$ 

Electrode	Co/Fe ratio	Overpotential @ 10 mA $\text{cm}_{\text{geo}}^{-2}$ (mV)	Tafel slope for OER ( $\text{mV dec}^{-1}$ )	Overpotential @ -10 mA $\text{cm}_{\text{geo}}^{-2}$ (mV)	Tafel slope for HER ( $\text{mV dec}^{-1}$ )
$\text{CoO}_x\text{H}_y/\text{TP}$	-	385	97	152	112
$\text{Co}_{65}\text{Fe}_{35}\text{O}_x\text{H}_y/\text{TP}$	1.86	335	57	150	75
$\text{Co}_{52}\text{Fe}_{48}\text{O}_x\text{H}_y/\text{TP}$	1.08	357	47	151	77
$\text{Co}_{47}\text{Fe}_{53}\text{O}_x\text{H}_y/\text{TP}$	0.89	375	71	198	67
$\text{FeO}_x\text{H}_y/\text{TP}$	0	481	92	292	94

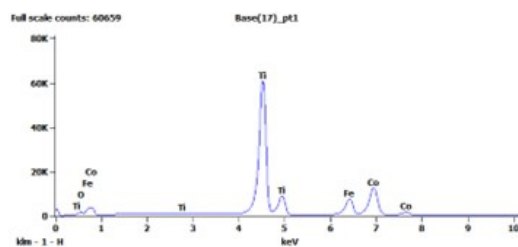
**Table S3** Operation conditions and performances of AEMWE using bifunctional  $\text{Co}_{65}\text{Fe}_{35}\text{O}_x\text{H}_y/\text{TP}$  and previously reported non noble metal-based electrodes

Catalyst (Anode and cathode)	MEA configuration		Electrolyte ( $\text{cm}^{-3} \text{min}^{-1}$ )	Operating temperature ( $^{\circ}\text{C}$ )	Current density @ 2.0 $V_{\text{cell}}$ ( $\text{A cm}^{-2}$ )	Reference
	Membrane	MEA fabrication				
$\text{Co}_{65}\text{Fe}_{35}\text{O}_x\text{H}_y/\text{TP}$	X37-50	CCS	1 M KOH (20)	50	0.61	This study
$\text{Fe}_{0.2}\text{Ni}_{0.8}\text{-P}_{0.5}\text{S}_{0.5}$	FAA-3-50	CCS	1 M KOH (50)	60	2.5	48
Ni foam	C-PVA-ABPBI	CCM	15 wt% KOH (-)	70	0.45	49
$\text{VCoCO}_x$	FAA-3-50	CCS	1 M KOH (-)	45	0.20	50
Ni foam	PF-41	-	20 wt% KOH (1)	60	0.8	51
Ni foam	PAEK-APMBI	-	10 wt% KOH (-)	60	0.64	52
Ni foam	FAA-3	-	10 wt% KOH (-)	60	0.03	53
$\text{NiCo}_2\text{O}_4\text{-HSp}$	PAni-1.03	CCS	1 M KOH (10)	50	0.4 @ 2 V	54
$\text{Ni}_{12}\text{P}_5/\text{Ni}_3(\text{PO}_4)_2$	YAB	CCS	1 M KOH (5)	50	0.36 @ 1.87 V	55
Ni	A201	CCS	1 M KOH (1)	50	0.19 @ 1.8 V	56
CoPNS	YAB	CCS	1 M KOH (5)	50	0.42 @ 1.8 V	57

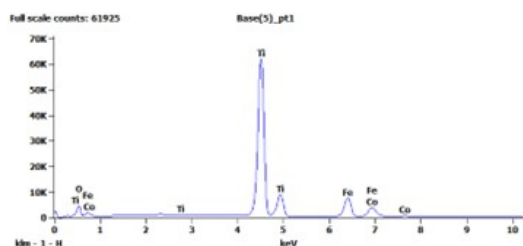
(a)



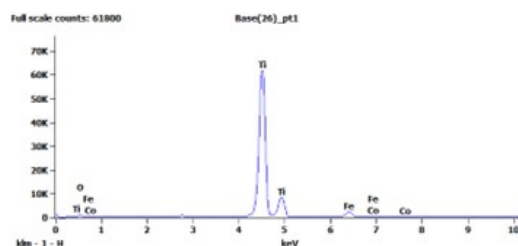
(b)



(c)



(d)



(e)

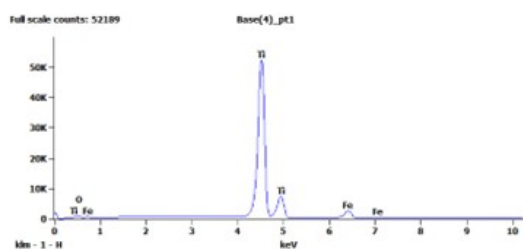


**Fig. S1** EDS spectra for (a)  $\text{CoO}_x\text{H}_y/\text{TP}$ , (b)  $\text{Co}_{65}\text{Fe}_{35}\text{O}_x\text{H}_y/\text{TP}$ , (c)  $\text{Co}_{52}\text{Fe}_{48}\text{O}_x\text{H}_y/\text{TP}$ , (d)  $\text{Co}_{47}\text{Fe}_{53}\text{O}_x\text{H}_y/\text{TP}$ , and (e)  $\text{FeO}_x\text{H}_y/\text{TP}$ .

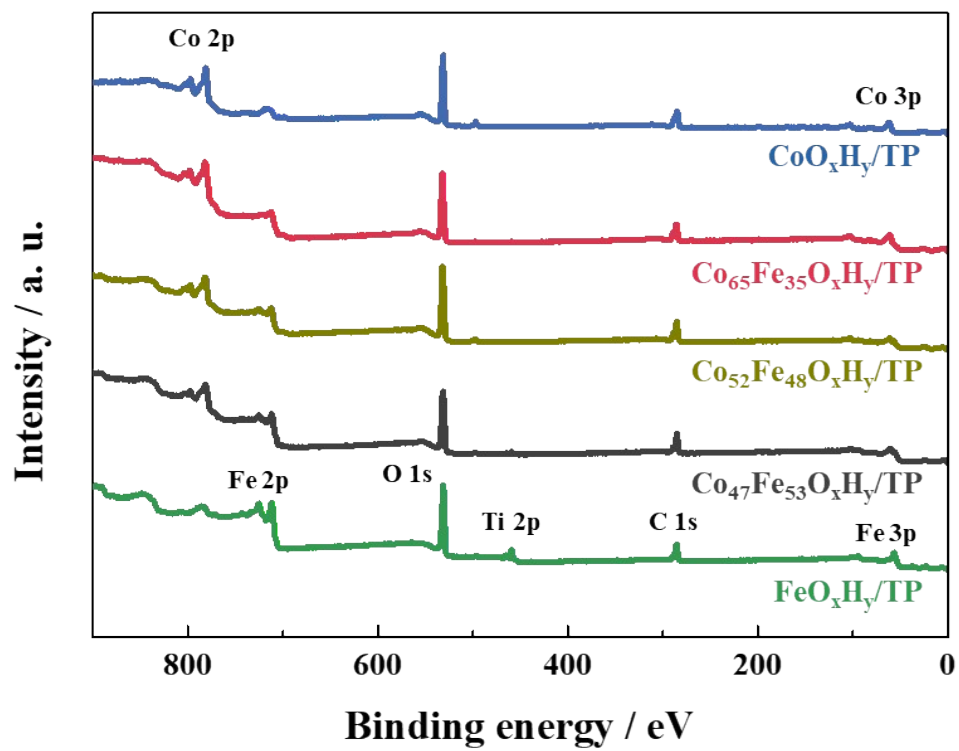


**Fig. S2** XPS spectra of  $\text{CoO}_x\text{H}_y/\text{TP}$ ,  $\text{Co}_2\text{Fe}_{1-z}\text{O}_x\text{H}_y/\text{TP}$ , and  $\text{FeO}_x\text{H}_y/\text{TP}$ .

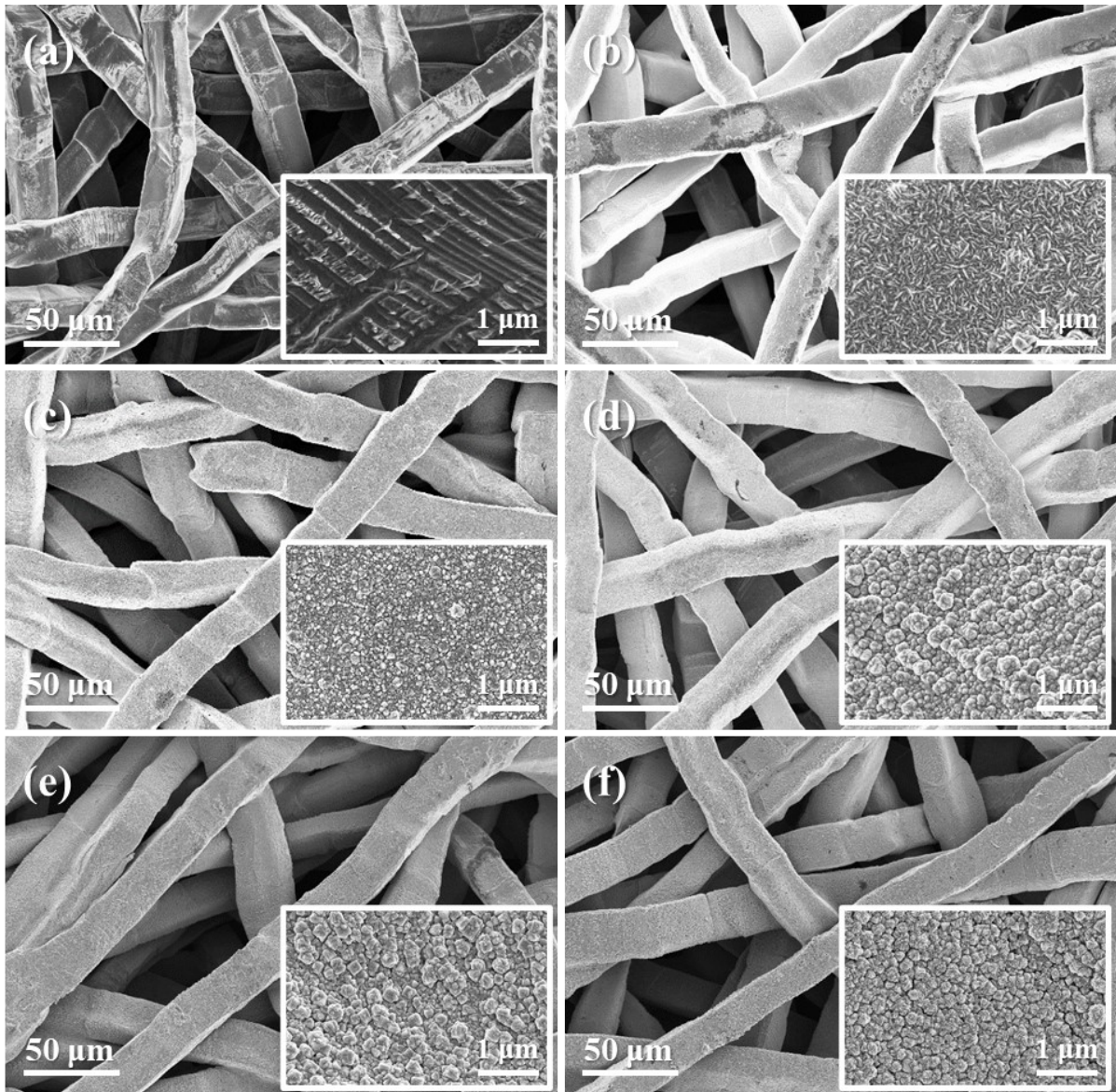


**Fig. S3** FESEM images of (a) bare TP, (b)  $\text{CoO}_x\text{H}_y/\text{TP}$ , (c)  $\text{Co}_{65}\text{Fe}_{35}\text{O}_x\text{H}_y/\text{TP}$ , (d)  $\text{Co}_{52}\text{Fe}_{48}\text{O}_x\text{H}_y/\text{TP}$ , (e)  $\text{Co}_{47}\text{Fe}_{53}\text{O}_x\text{H}_y/\text{TP}$ , and (f)  $\text{FeO}_x\text{H}_y/\text{TP}$ . Insets: corresponding images at a higher magnification.

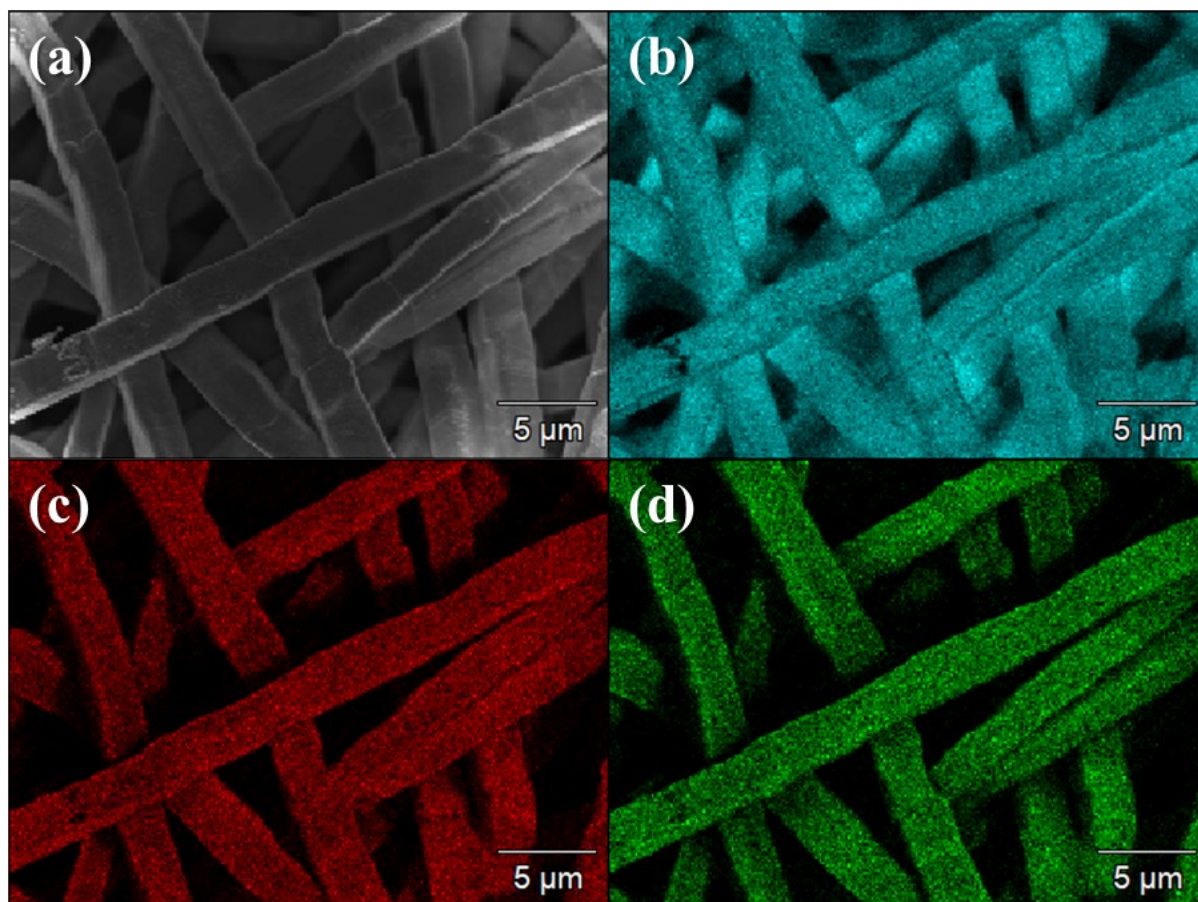


**Fig. S4** EDS mapping of  $\text{Co}_{65}\text{Fe}_{35}\text{O}_x\text{H}_y/\text{TP}$ . (a) FESEM image and elemental mapping images of: (b) O, (c) Co, and (d) Fe.

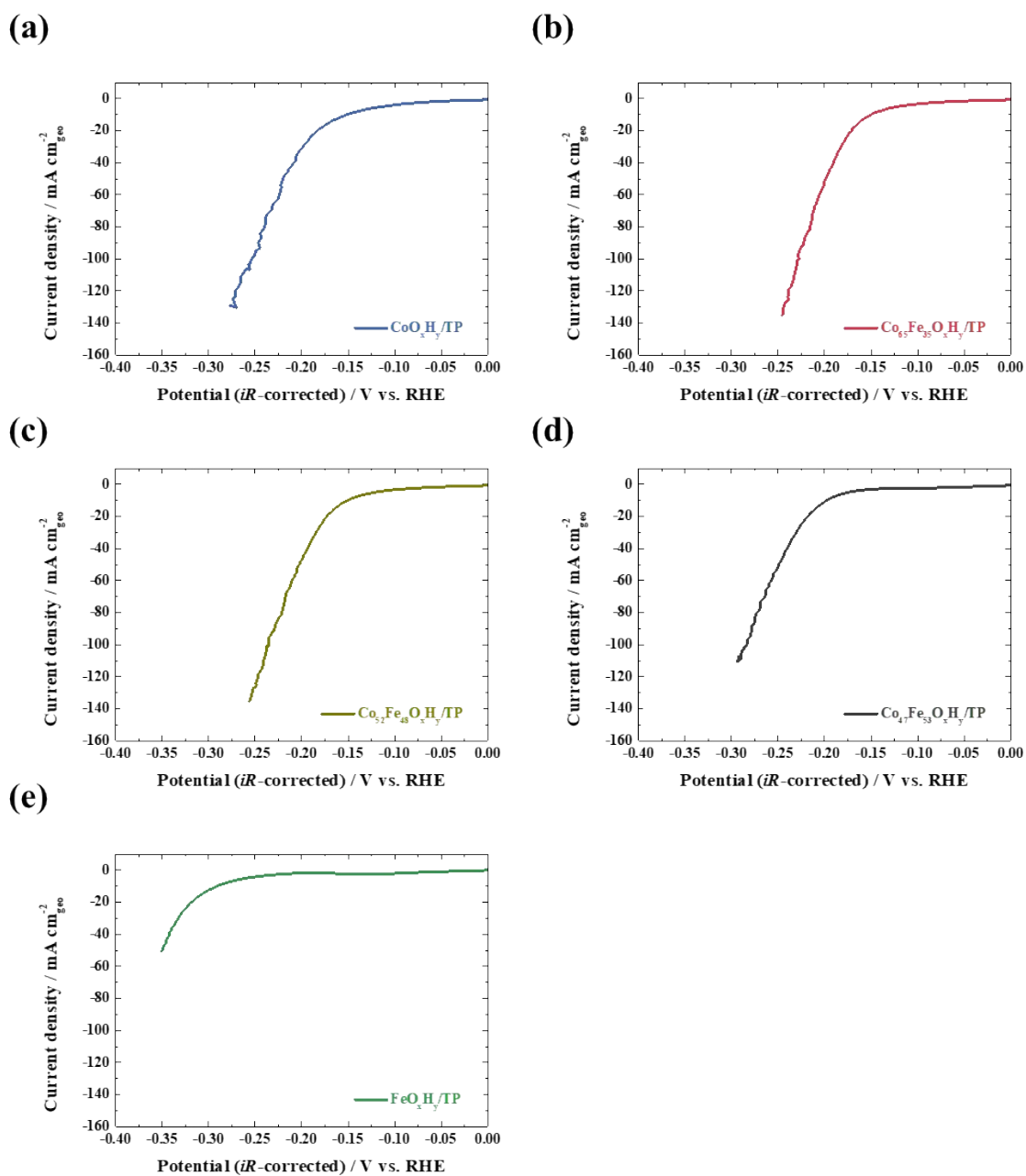


**Fig. S5** Polarization curves of HER activity at 5 mV/s in 1.0 M KOH: (a) CoO<sub>x</sub>H<sub>y</sub>/TP, (b) Co<sub>65</sub>Fe<sub>35</sub>O<sub>x</sub>H<sub>y</sub>/TP, (c) Co<sub>52</sub>Fe<sub>48</sub>O<sub>x</sub>H<sub>y</sub>/TP (d) Co<sub>47</sub>Fe<sub>53</sub>O<sub>x</sub>H<sub>y</sub>/TP, and (e) FeO<sub>x</sub>H<sub>y</sub>/TP.



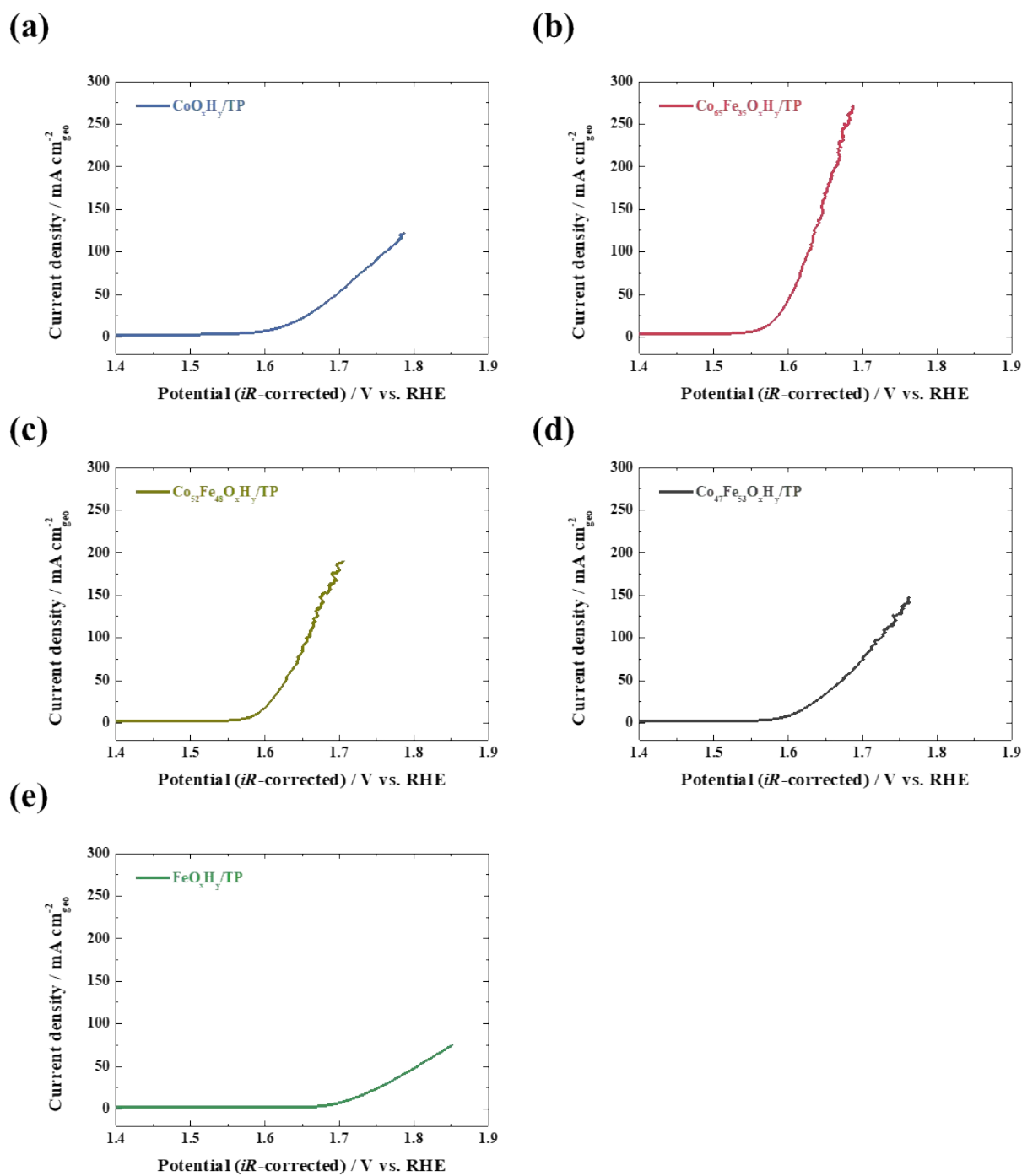


**Fig. S6** Polarization curves of OER activity at 5 mV/s in 1.0 M KOH: (a)  $\text{CoO}_x\text{H}_y/\text{TP}$ , (b)  $\text{Co}_{65}\text{Fe}_{35}\text{O}_x\text{H}_y/\text{TP}$ , (c)  $\text{Co}_{52}\text{Fe}_{48}\text{O}_x\text{H}_y/\text{TP}$  (d)  $\text{Co}_{47}\text{Fe}_{53}\text{O}_x\text{H}_y/\text{TP}$ , and (e)  $\text{FeO}_x\text{H}_y/\text{TP}$ .

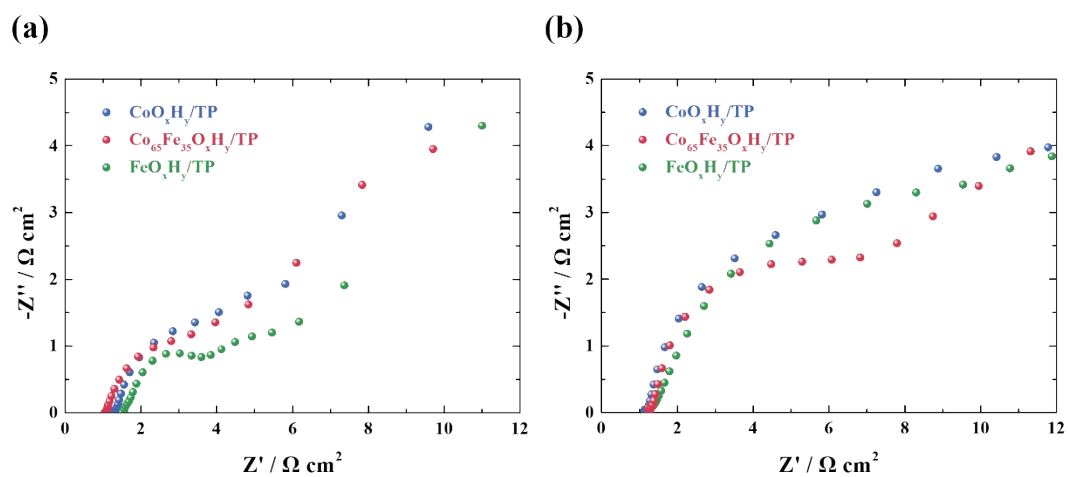


**Fig. S7** Nyquist plot of each electrode measured at current density of (a)  $10 \text{ mA cm}^{-2}$  for OER, and (b)  $-10 \text{ mA cm}^{-2}$  for HER.

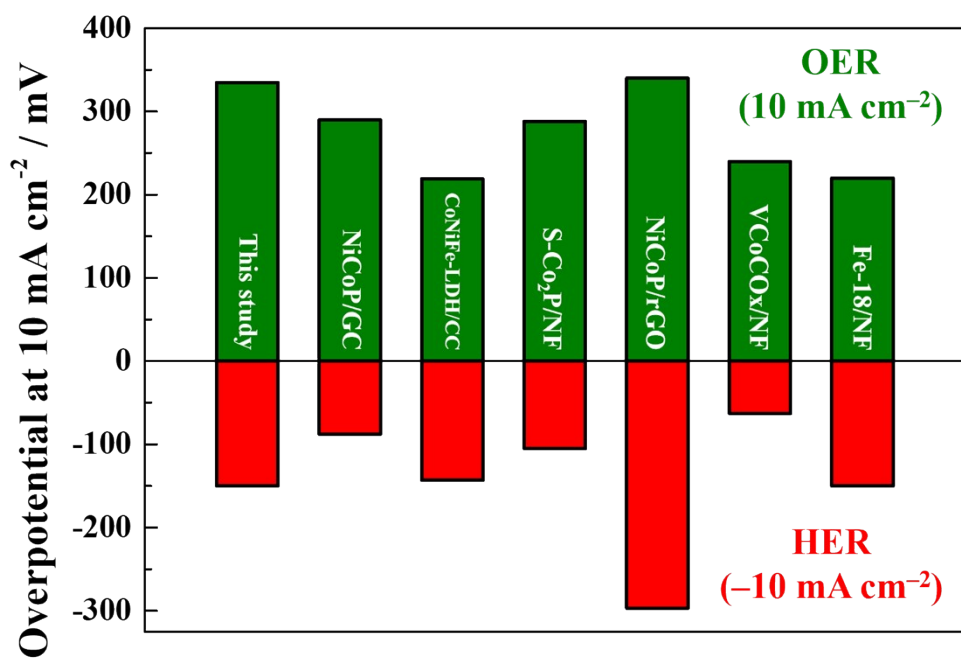
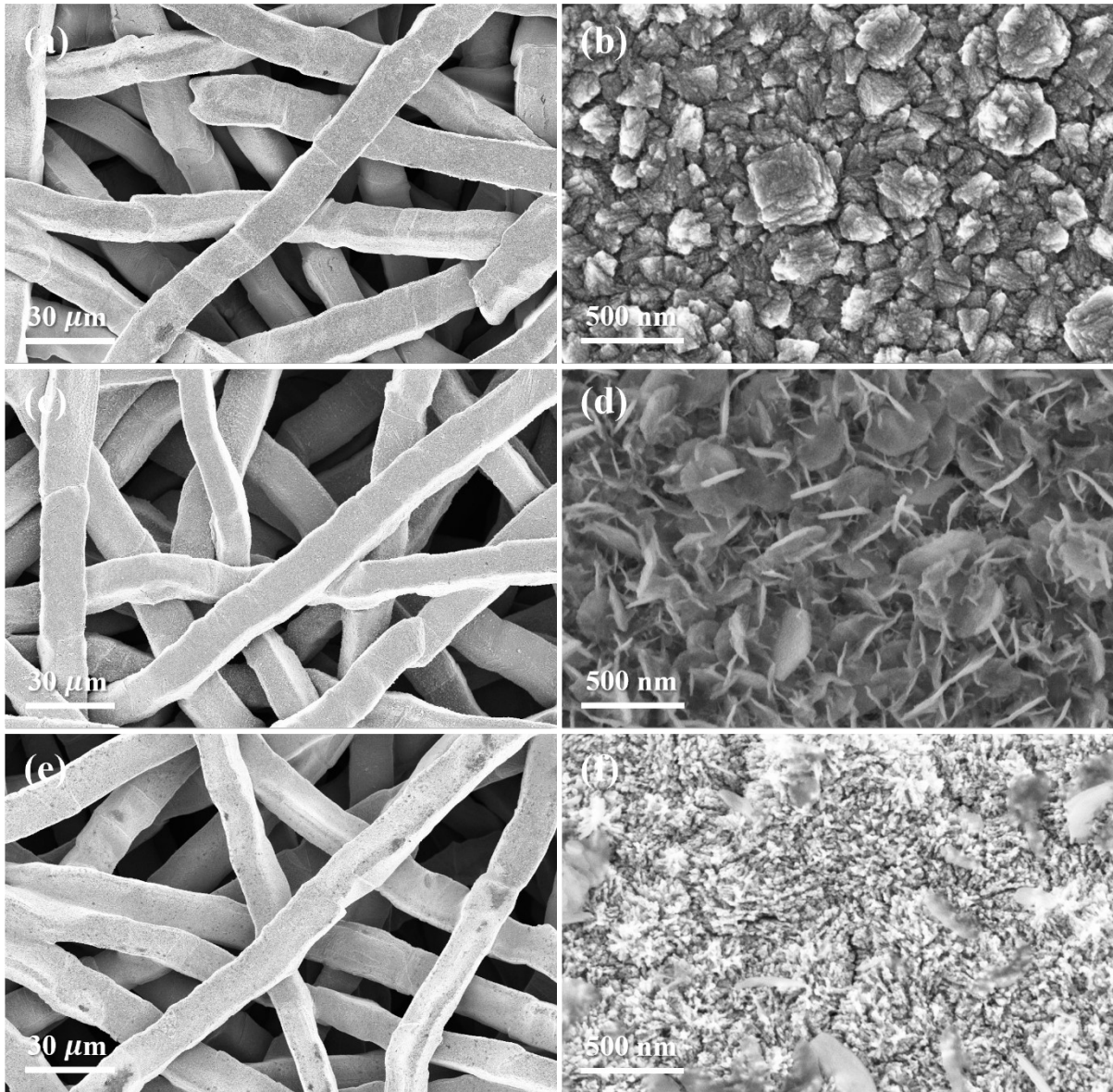
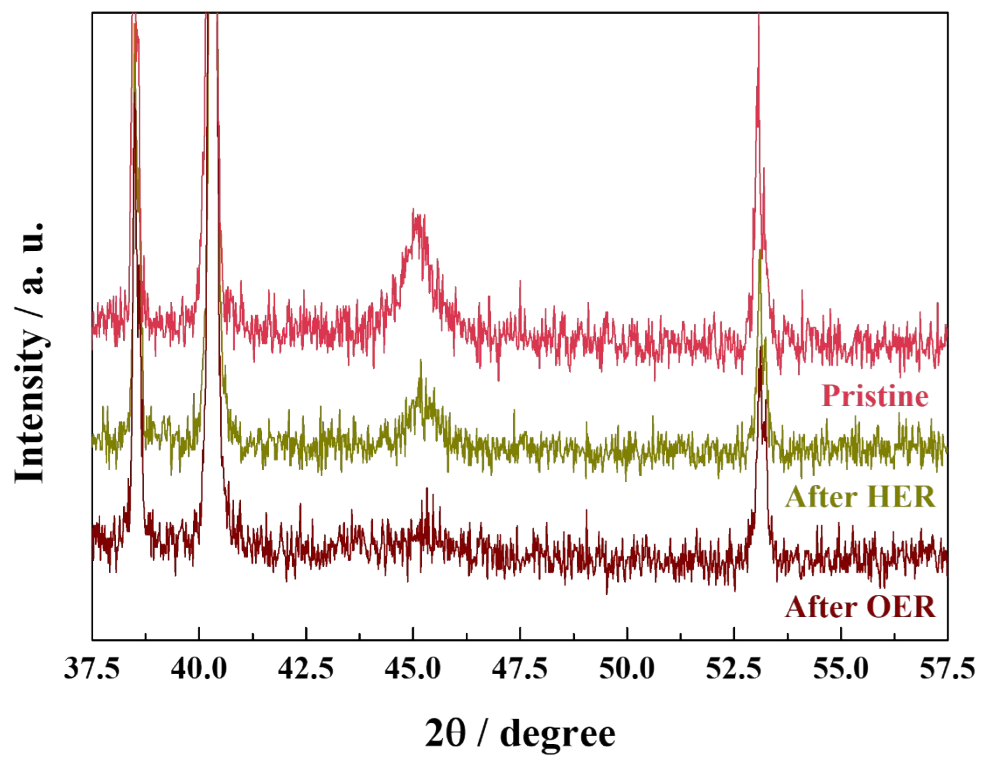


Fig. S8 Comparison of OER/HER overpotential in alkaline condition.



**Fig. S9** FESEM images of  $\text{Co}_{65}\text{Fe}_{35}\text{O}_x\text{H}_y/\text{TP}$  electrode. (a-b) pristine  $\text{Co}_{65}\text{Fe}_{35}\text{O}_x\text{H}_y/\text{TP}$ , (b) (c-d)  $\text{Co}_{65}\text{Fe}_{35}\text{O}_x\text{H}_y/\text{TP}$  after OER long-term stability test, (e-f)  $\text{Co}_{65}\text{Fe}_{35}\text{O}_x\text{H}_y/\text{TP}$  HER long-term stability test.



**Fig. S10** XRD patterns of the  $\text{Co}_{65}\text{Fe}_{35}\text{O}_x\text{H}_y/\text{TP}$  after HER/OER stability test.

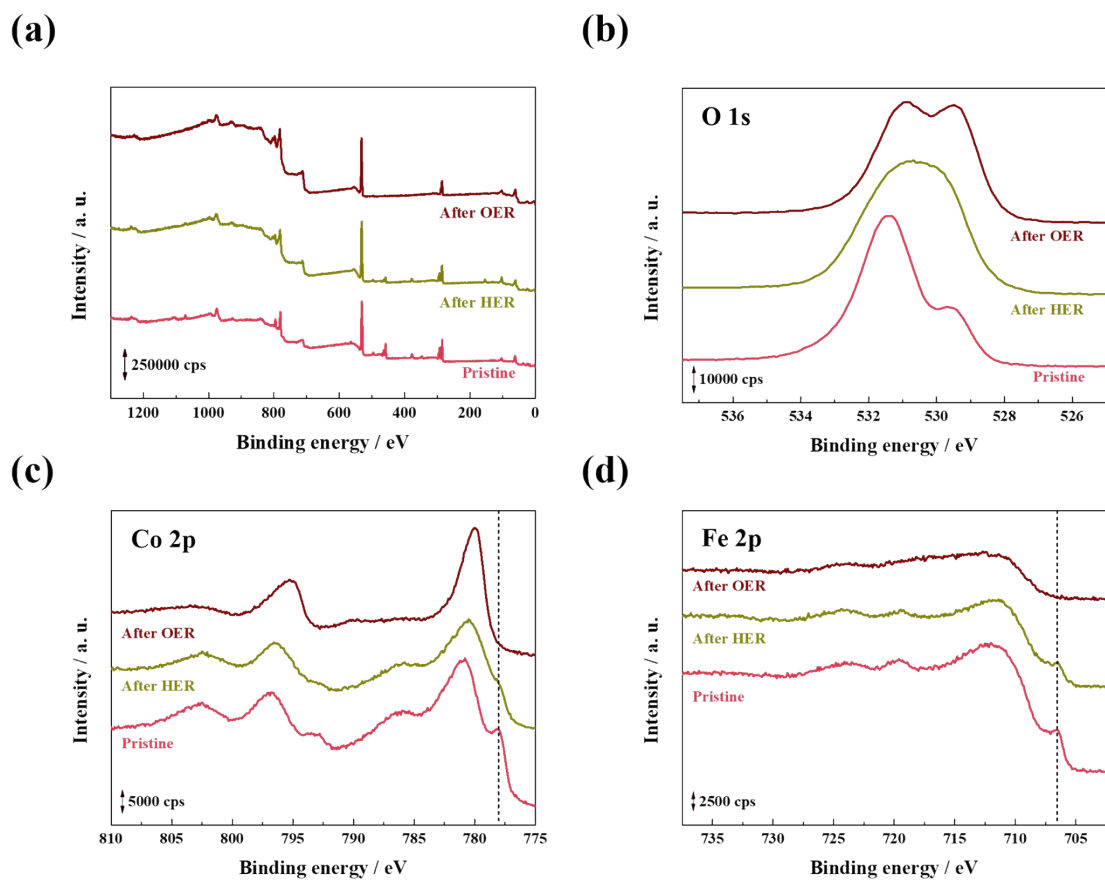


**Fig. S11** XPS spectra of pristine and after stability test for (a) survey peaks, (b) O 1s, (c) Co 2p, and (d) Fe 2p.

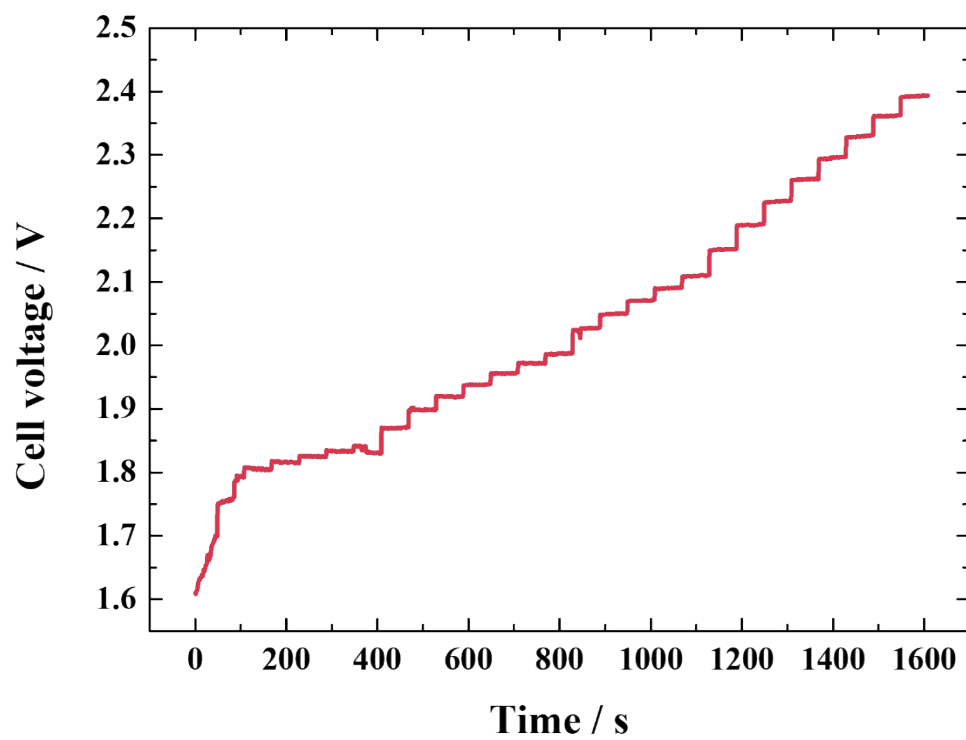


**Fig. S12** Chronoamperometric curves for the AEMWE with bifunctional  $\text{Co}_{65}\text{Fe}_{35}\text{O}_x\text{H}_y/\text{TP}$ .

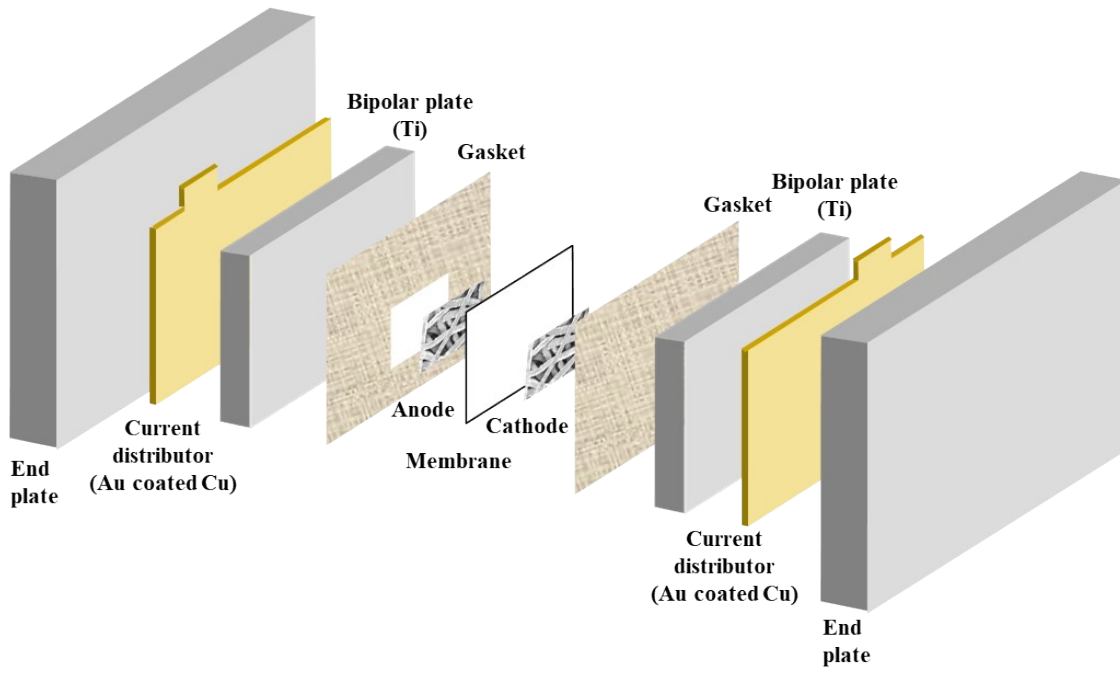


**Fig. S13** Configuration of AEMWE single-cell.